A Dynamic Mechanical and Dielectric Relaxation Study of PP-g-MAH/ Clay Nanocomposites

Amol Ridhore[1] and J.P. Jog*[,2]

[1]*Department of Chemical Engineering, Indian Institute of Technology Bombay, Mumbai-400076, India*

[2]*Polymer Science and Engineering Division, National Chemical Laboratory, Dr. Homi Bhabha road, Pune-411008. India*

Abstract: The relaxations in maleic anhydride grafted polypropylene (PPgMAH) and its nanocomposite based on organically modified layered silicates were investigated using dynamic mechanical thermal analysis and dielectric relaxation spectroscopy. The results of dynamic mechanical thermal analysis showed that the incorporation of clay in the polymer matrix resulted in two relaxations corresponding to the glass transition and a high temperature transition. In nanocomposites, the incorporation of clay resulted in reduction of the loss modulus peak area for the glass transition peak suggesting decreased content of mobile amorphous phase. An increase in the area of the high temperature transition was noted and associated with the presence of rigid amorphous phase. The dielectric measurements indicated presence of a relaxation at high frequency side for the PPgMAH whereas in nanocomposite two relaxations in the low frequency side were observed namely MWS relaxation or the interfacial polarization of the polymer and clay followed by α_{RAP} relaxation due to relaxation of rigid amorphous phase. The presence of rigid amorphous phase was attributed to the strong bonding between the MAH groups of PPgMAH and the clay surface.

Keywords: PPgMAH, rigid amorphous phase, dielectric spectroscopy, nanocomposites.

1. INTRODUCTION

Polymer layered silicate nanocomposites have shown great promise in technological sector since they offer significant enhancement in properties. The nanocomposites of polypropylene with organically modified layered silicates and functionalized polypropylene by melt intercalation technique are well known in the field of polymer nanotechnology [1-5]. These nanocomposites are also interesting from research point of view and many attempts have been made to explore the interaction of these clays with polymers using various preparation and characterization techniques [6-10]. As the clays are hydrophobic, major problem in developing these nanocomposites is of dispersing clay in non-polar polymers such as polypropylene (PP). As a result number of studies on clay modification and use of different compatibilizers have been reported [11-16]. Depending on the state of dispersion of clay platelets in the polymer matrix, the nanocomposites can be classified as intercalated or exfoliated nanocomposites [17]. The intercalated clay-polymer nanocomposites have clay layers dispersed in a polymer matrix with larger inter gallery spacing associated with the insertion of polymer chains into the gallery. In some cases, nanocomposites exhibit exfoliated structure, wherein the silicate layers are completely delaminated and dispersed randomly in the polymer matrix. However in practice, most of the times a combination of intercalated and exfoliated structures is observed and the extent of intercalation or exfoliation depends on the polymer clay interaction and the processing conditions.

The reported literature on PP/clay nanocomposites is mostly on three phase system namely PP-compatibilizer-clay. The dispersion of the clay and the properties of these nanocomposites mostly depend on the type, amount of the compatibilizer used and also the modification of clay. The interaction of the compatibilizer is well understood by studying two phase systems consisting of the compatibilizer and the clay. There have been few reports on the compatibilizer/clay systems [18-20]. However, the results are specific to the compatibilizer and the clay used in the study. Our earlier work on dynamics of polymer/clay nanocomposites have shown that the molecular dynamics of the polymer is significantly affected by the clay dispersion [21, 22].

In this communication we present a study molecular dynamics of a two phase system comprising of a compatibilizer (Fusabond®M-613-05) and clay (Cloisite® 20A) using dynamic mechanical thermal analysis and dielectric relaxation spectroscopy.

2. EXPERIMENTAL

2.1. Materials

Maleic anhydride grafted Polypropylene (PPgMAH); grade Fusabond®M-613-05 of MFR 49 g/10 min (MFR method =190ºC/10min) with 0.5-wt % maleic anhydride (MAH) obtained from DuPont Canada was used for the present investigation. Cloisite® 20A (modified with, Dimethyl dehydrogenated tallow quaternary ammonium chloride) was supplied by Southern Clay Products, Texas, U.S.A.

*Address correspondence to this author at the Polymer Science and Engineering Division, National Chemical Laboratory, Dr. Homi Bhabha road, Pune-411008. India; Tel: +91 20 25902176; Fax: +91 20 25902618; E-mail: jp.jog@ncl.res.in

2.2. Preparation of Nanocomposite

The organoclay Cloisite 20A and PPgMAH were dried at 100 º C for 24 hrs in a vacuum oven prior to compounding. Melt mixing of the samples was performed in an internal mixer (Thermo-Haake Polylab system, Rheomix 600, capacity 50 gms) equipped with two roller rotors. A dry batch containing PPgMAH & Cloisite 20A components were pre-mixed before introduction into the internal mixer. The compounding was done under the following conditions: rotor speed 100 rpm, mixing time 5 min and mixer temperature 200 º C. The organoclay content in polymer matrix was 5 % by weight. For comparison, the base polymer (PPgMAH) without organoclay was also prepared by melt mixing under the same conditions.

Film samples with a thickness of 1 mm were prepared using a compression molding press and were further used for characterization. PPgMAH is highly hygroscopic material having tendency to absorb environmental moisture, which greatly affects its electrical properties [18]. Samples were therefore stored in desiccators prior to characterization.

2.3. Characterization Methods

2.3.1. Wide Angle X-Ray Diffraction (WAXD)

The intercalation of polymer in clay layers was confirmed by wide angled X-ray diffractometer (WAXD). The d_{001} peak of the clay was monitored in the nanocomposites and the shift in the d-spacing in the nanocomposite was evaluated. WAXD patterns of the samples were recorded at room temperature using a Rigaku D/Max 2500 unit equipped with CuK$_\alpha$ radiation in reflection mode with a wavelength of 0.154 nm. Spectra were obtained in the range $2\theta = 2$–$12º$ with a step scanning rate of $4º$ min^{-1}. The basal spacing of the clay was estimated from peak in the XRD pattern using Bragg's law.

2.3.2. Differential Scanning Calorimetry (DSC)

The measurement of the degree of crystallinity of PPgMAH and its nanocomposite was carried out by using TA instrument, Q10, DSC (USA). Test was conducted by placing sample in sealed aluminum pan over a temperature range of -60 to 200 ºC. A controlled heating rate and cooling rate was maintained at 10 ºC/min. The tests were carried out in inert Nitrogen atmosphere. The melting point (T_m) and heat of fusion were determined from the heating scans. The percentage crystallinity (X_c) of PPgMAH and its nanocomposite (i.e. PPgMAH20A) was estimated from the heat of fusion (ΔH_f) using heating scan as follows:

$$X_c(\%) = \frac{\Delta H_f}{\Delta H_0(1 - \phi_{Clay})} \times 100 \qquad (1)$$

Where ΔH_0 designated as the melting enthalpy of 100 % crystalline polypropylene [23] and ϕ_{Clay} indicates the fraction of Cloisite 20 A in the nanocomposite.

2.3.3. Dynamic Mechanical Thermal Analysis (DMTA)

Dynamic mechanical properties of PPgMAH/Clay nanocomposites were measured using a Dynamical mechanical thermal analyzer, DMTA IV Rheometric scientific (Piscataway, NJ, USA) in single cantilever bending mode with a strain of 0.02%. Temperature range from −100 to 100 ºC and

the heating rate of 5 ºC/min was used for the measurements. The test was performed at 1 Hz frequency. The size (length × width × thickness) of the test samples was $20 \times 6 \times 1mm^3$.

### 2.3.4. Dielectric Relaxation Spectroscopy (DRS)

Dielectric relaxation spectroscopy (DRS) measurements were performed on Novocontrol Alpha analyzer (*Germany*) in the frequency range of 10^{-2} to 10^6 Hz and temperature range of 40 to 100 ºC in 10 ºC steps. The temperature was well controlled by Novotherm system with accuracy of 0.2 ºC. Dielectric measurements were carried out using gold-coated copper electrodes of diameter 20 mm. The sample of thickness 1 mm & diameter 25mm was used.

3. RESULTS & DISCUSSION

Long chain organic surfactant on organoclay sheets contribute to expand clay galleries during compounding process by allowing functional polymeric chains to enter the galleries and majority of functional macromolecular chain found to be in close environment of clay sheets. However, process of formation of intercalated or exfoliated structure is completely governed by the thermodynamics. Extent of intercalation or exfoliation governs the structure and morphology.

3.1. Structure & Morphology

The structure of the nanocomposite was studied using X-ray diffraction. Fig. (**1**) illustrates the XRD scans of the organically modified clay Cloisite 20 A and its nanocomposite with PPgMAH. The clay exhibits a well defined d_{001} diffraction peak with a d-spacing of 2.4 nm. In nanocomposite, a broad peak is observed at lower angle instead of a well defined peak confirming the intercalation of PPgMAH in clay layers. A broad peak with reduced intensity is observed in nanocomposite. The broadening of the peak with reduced intensity suggests good dispersion of clay layers with partially exfoliation in polymer matrix [24, 25].
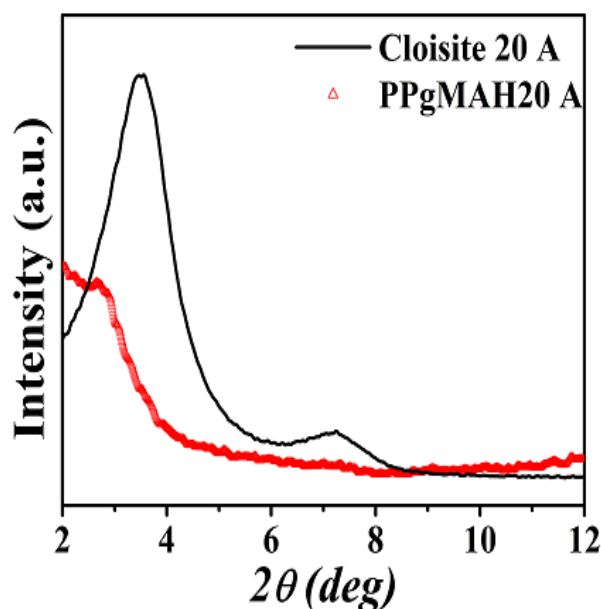
Fig. (1). Wide angle X-ray diffraction patterns for Cloisite 20A and PPgMAH20A.

3.2. Differential Scanning Calorimetry (DSC)

The crystallization and melting behavior of nanocomposite and its base polymer was studied using DSC. The melting temperature and the degree of crystallinity as determined from the heat of fusion are presented in Table **1**. The values of heat of fusion were normalized with respect to the polymer content. All the parameters showed marginal changes as a result of incorporation of clay in PPgMAH matrix.

Table 1.   Comparison of DSC Data for PPgMAH and PPgMAH20A

| Compositions	T_m (° C)	ΔH_f (Jg^{-1})	X_c (%)
PPgMAH	158.2	99.3	47.9
PPgMAH20A	158.0	96.6	46.6

T_m, temperature of melting peak; ΔH_f, enthalpy of fusion; X_c, percentage.

3.3. Dynamical Mechanical Spectroscopy

Dynamic mechanical thermal Analysis (DMTA) is an excellent tool to probe different transitions in polymers under influence of frequency and temperature. The storage modulus is related to the stiffness of the material and measures the elastic response of the polymer. The loss modulus denotes the energy dissipated by the system in the form of heat and measures the viscous response of the polymer material. The damping factor (tan δ) is ratio of loss modulus to storage modulus. In PPgMAH over the entire temperature range, two main mechanical relaxation processes are reported, namely high temp α_c relaxation, related to the crystalline fraction present and a α process, related to the glass-rubber transition relaxation [26]. In DMTA measurements, the transition from glassy to rubbery state is purely kinetic phenomenon and is governed by measuring time & applied frequency. In the present experiments the applied frequency was 1 Hz.

The relaxations in PPgMAH and PPgMAH /clay nanocomposites are depicted in Fig. (**2**). In the loss modulus spectra of the base polymer, two well-defined relaxations are discernible and a broad peak is observed at low temperature. The peak at about 9 ºC corresponds to the glass transition temperature (α) of PP while the peak at about 72 ºC (α_c) is related to the relaxation of crystalline phase. The low temperature peak is attributed to the local motions in the amorphous phase. In nanocomposites, two peaks are discernible. The peak corresponding to the glass transition remains at about the same temperature with lower intensity. Since the area under the glass transition peak is proportional to the mobile amorphous phase, reduced area of the glass transition indicates a decrease in the mobile amorphous phase in nanocomposite. DSC results showed that the crystallinity of the nanocomposites is almost the same as the base polymer. This suggests equal amorphous content for the base polymer and the nanocomposite and as a result the loss modulus peak, which corresponds to mobile amorphous phase (α), should have remained unchanged. However, the lower value of area under the loss modulus peak indicates a lower mobile amorphous fraction in the nanocomposites. Thus the observed decrease in loss modulus value of nanocomposites compared to polymer reveals a decrease in content of mobile amor-

phous phase and presence of rigid amorphous phase (α_{RAP}) with reduced chain mobility [27]. The damping in polymeric materials is sensitive of segmental mobility of the polymer chain and in nanocomposites it is indicative of the interfacial interaction between the polymer and the filler as the chain mobility of the polymer close to the filler surface differs from that of the bulk polymer [28]. Strong interfacial interaction between the polymer and the filler tends to restrict the polymer mobility thereby reducing the damping. These results confirm the presence of strong interfacial interaction between clay and polymer, which leads to the formation of rigid amorphous phase.
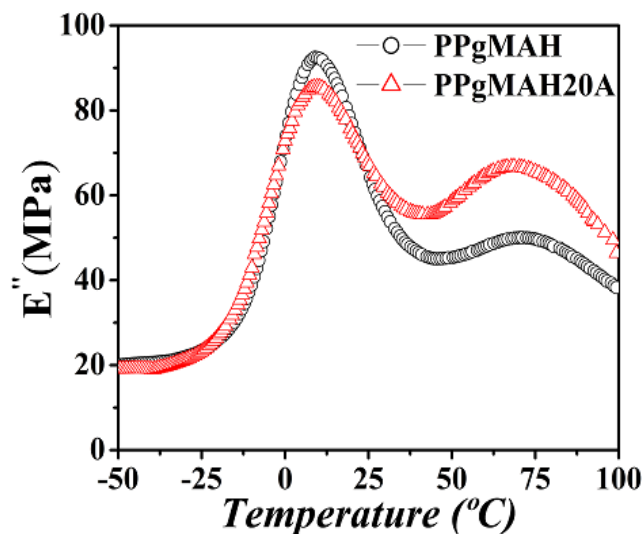
Fig. (2). Plot of temperature dependencies of Loss modulus curves for PPgMAH and PPgMAH20A.

The crystalline peak (α_c) is found to be about the same temperature with a higher intensity and correspondingly larger area. As this peak corresponds to the relaxation of crystalline phase, and crystallinity values of base polymer and the nanocomposite are comparable, the increased area of this peak could be ascribed to the relaxation of rigid amorphous phase which takes place in the vicinity of the crystalline relaxation.

In summary, the dynamic mechanical analysis shows that the incorporation of clay results in decreased loss modulus values indicating reduced fraction of mobile amorphous phase. The results also confirmed the presence of a rigid amorphous phase, which displayed a relaxation at higher temperature than the glass transition temperature and in the vicinity of crystalline (α_c) relaxation.

3.4. Dielectric Relaxation Spectroscopy (DRS)

Dielectric relaxation spectroscopy has been widely used in polymer relaxation analysis and has the advantage over dynamic mechanical thermal analysis methods is, that it covers much wider frequency ranges. The dielectric relaxation spectroscopy (DRS) measures the response of electric dipoles to an oscillating electric field. The real and imaginary parts of the complex dielectric function are calculated. In the molten state, dipole moments on the amorphous polymer chains are free to move. Once crystals are formed, mobility

of the dipoles is reduced and this phenomenon can be studied by reverse process of disturbing ordered structure and monitored as a shift in the relaxation frequency spectrum. Complementary structural information is needed to determine the size of crystals, their arrangement and perfection, and the overall degree of crystallinity. This study of polymers as a function of frequency and temperature can be used to elucidate the effects of intermolecular co-operative motions and hindered dielectric rotations [29, 30]. In case of polymer/clay nanocomposite, DRS is used to probe role of confined (intercalated) & exfoliated structure formed in nanocomposite apart from molecular rearrangement [28, 31-33].

Fig. (**3**) shows the room temperature dielectric loss spectra for base polymer (PPgMAH) and its nanocomposite (PPgMAH20A). As evident from the Fig. (**3**) only one relaxation is observed in these samples. For base polymer a high frequency relaxation is observed at about 4.86×10^{2} Hz which can be ascribed to the sub-glass transition relaxation (β -relaxation) [34], and is related to the presence of polar maleic anhydride groups present in the polymer [18]. The α transition corresponding to the glass transition is not detected for the base polymer. This observation is similar to those reported by Bohning *et al*. [18].
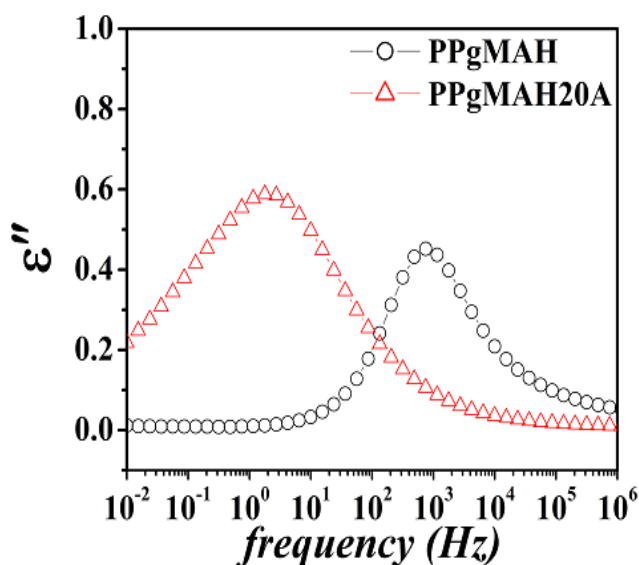
Fig. (3). Dielectric loss spectra position at 40 ºC of PPgMAH and PPgMAH20A.

For the nanocomposite a low frequency relaxation at about 5.61×10^{-2} Hz is noted. The low frequency relaxation observed in the nanocomposite can be assigned to the MWS type relaxation. In polymer clay nanocomposites, this additional process is observed at low frequency side of spectrum termed as interfacial polarization process due to the blocking of charge carriers at internal phase boundaries. Generally, such an interfacial polarization process is caused by blocking of charge carriers at internal surfaces or interfaces of different phases having different value of dielectric constant [21, 22]. Fig. (**3**) also illustrates that the sub-glass transition (β) relaxation associated with dipolar fluctuation of maleic anhydride groups is absent in the nanocomposite. This could be due to fact that functional groups bonded to organic content of silicate layers.

The temperature dependence of these two relaxations observed in base polymer and in the nanocomposite is studied and the results are presented in Figs. (**4** and **5**). We can see that in the base polymer (Fig. **4**) intensity of dielectric loss peak with temperature almost remains constant and the peak shifts to higher frequency side. The shape of curve also remains unchanged over entire temperature range. β relaxation appeared in amorphous domain of polymer is insensitive to morphological changes like crystallinity or other constrains [35].

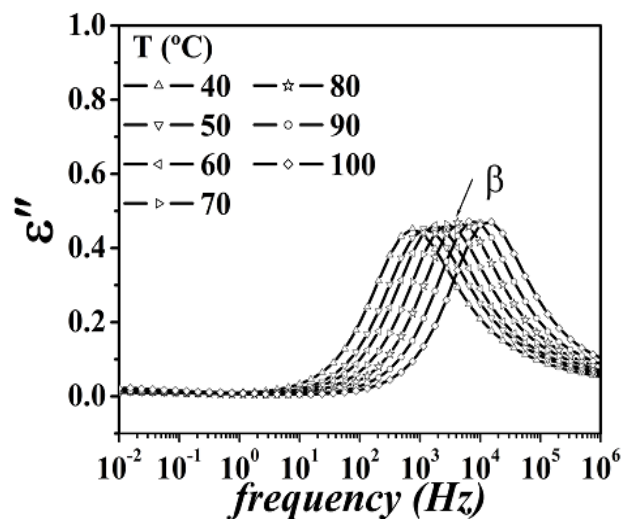**Fig. (4).** Dielectric loss (ε″) as a function of logarithmic frequency for PPgMAH from 40-100 ºC.

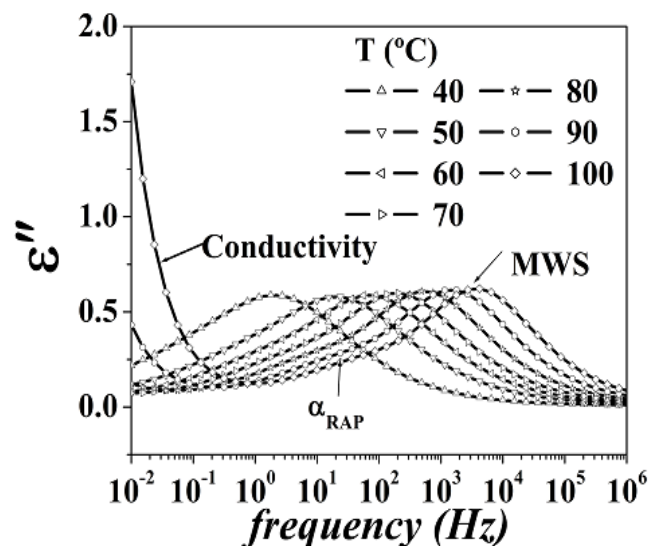**Fig. (5).** Dielectric loss (ε″) as a function of logarithmic frequency for PPgMAH20A from 40-100 ºC.

In case of nanocomposite observed MWS relaxation however is found to be a broad and cover wide frequency range. This MWS relaxation is coupled with another relaxation at high temperature. Fig. (**6**) illustrates the MWS relaxation peak at 80 ºC. As can be seen, a shoulder at low frequency tail of the MWS relaxation is clearly visible. This data is further analyzed using Havriliak-Negami equation. Fig. (**6**) shows the Havriliak-Negami fit for the dielectric loss

data at 80 ºC. It can be seen that the broad peak can be resolved into two peaks. The faster relaxation corresponds to the MWS relaxation while slower relaxation can be attributed to the relaxation of the constrained amorphous phase or the rigid amorphous phase (α_{RAP}), The broad nature of this peak represents a broad distribution of relaxation times. In case of clay nanocomposite, it can be visualized that the clay polymer interaction can result in different dynamics or relaxation times. The relaxation of rigid amorphous phase has been reported in many semi-crystalline polymers as well as nanocomposites [36, 37].
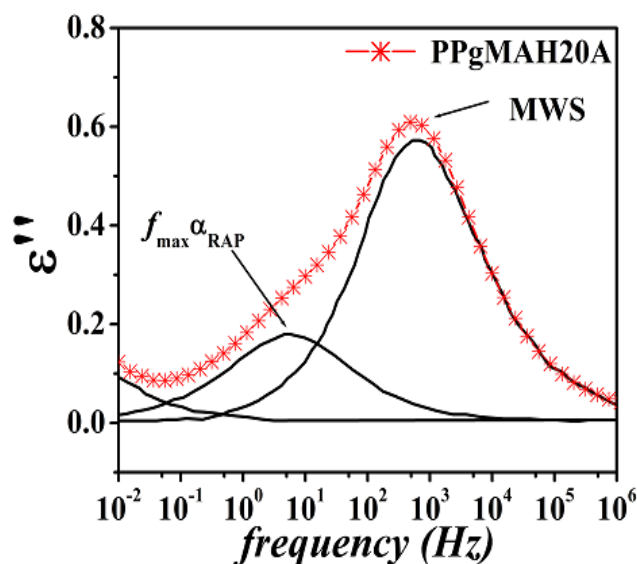

Fig. (6). Fitted curve using Havriliak-Negami equation (H-N) at temperature 80 ºC for PPgMAH20A.

Fig. (**7**) represents the temperature dependence of frequency associated with peak maxima ($f_{max} = \frac{1}{2} \pi \tau_{max}$) of the various relaxation processes. Subglass transition process observed only in PPgMAH follows Arrhenius behavior with
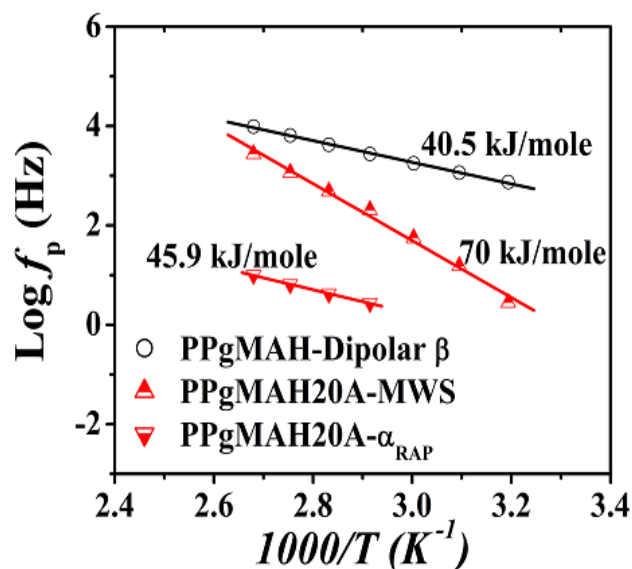

Fig. (7). Dependency of frequency of maximum loss of different relaxation as a function of reciprocal temperature for PPgMAH and PPgMAH20A.

activation energy of 40.5 kJ/mole. The activation energy associated with interfacial relaxation also follows Arrhenius behavior with activation energy of 70 kJ/mole. It is speculated that rigid amorphous phase is clay dominated and these clay-polymer interface loosing integrity with time-temperature scale. This rigid amorphous phase associated transition, observed after 50ºC can be seen as Arrhenius behavior with activation energy of 45.9 kJ/mole. Thus the results of dielectric relaxation are consistent with the results of dynamical mechanical thermal analysis.

4. DISCUSSIONS

It is well known fact that relaxation mechanism substantially change with type and amount of maleic anhydride groups and their distribution on chain. Bohning *et al.* studied nanocomposites of PPgMAH (0.6 % MAH content) with two different grades of clay prepared by melt blending technique [18]. They have shown that only one relaxation corresponding to the β-relaxation could be observed in the dielectric relaxation and the activation energy for β -relaxation was 47.3kJ/mol. With increasing temperature the peak frequency shifted to lower values. It was also reported that the α - process corresponding to the segmental dynamics connected with the glass transition was not detected due to the low concentration of grafted MAH groups. In the present study, our observations of single relaxation (β-relaxation) and absence of α-relaxation are similar to those reported by Bohning *et al*.

Wang *et al.* have studied nanocomposites with different amount of clay prepared by melt blending technique and also by solution blending technique [19, 20]. They analyzed these nanocomposites using DMA and DRS techniques and observed two relaxations in dynamical mechanical analysis (DMA) and only a single high-temperature process in broadband dielectric measurements. The observed relaxation was attributed to the Maxwell- Wagner-Sillars (MWS) polarization. These observations are similar to our results.

CONCLUSIONS

In this work PPgMAH and its nanocomposite (PPgMAH20A) containing Cloisite 20A, were processed by melt intercalation techniques. The dynamic mechanical thermal analysis showed decrease in the mobile amorphous phase and presence of rigid amorphous phase as evidenced by the relaxation at high temperature. The results of dielectric spectroscopy showed a β relaxation in PPgMAH at room temperature ascribed to the molecular fluctuations of MAH groups and no peak corresponding to the glass transition temperature or α transition. In nanocomposite the β relaxation is not visible in the experimental window while a relaxation corresponding to interphase polarization (MWS relaxation) is observed. At higher temperatures an additional peak is observed as evidenced by the shoulder on the low frequency side of the MWS. This relaxation is attributed to the rigid amorphous phase, which arises due to restricted chain mobility of polymer chains at the clay surface.

ACKNOWLEDGEMENT

REFERENCES

[1] Varela, C.; Rosales, C.; Perera, R.; Matos, M.; Poirier, T.; Blunda, J.; Rojas, H. Functionalized polypropylenes in the compatibilization and dispersion of clay nanocomposites. *Polym. Composit.,* **2006***, 451-458.

[2] Velasco, J.I.; Ardanuy, M.; Realinho, V.; Antunes, M.; Fernandez, A.I.; Gonzalez-Pena, J.I.; Rodriguez, M.A.; DeSaja, J.A. Polypropylene/Clay nanocomposites: Combined effects of clay treatment and compatibilizer polymers on the structure and properties. *J. Appl. Polym. Sci.,* **2006***, 102*, 1213-1223.

[3] Liu, X.; Wu, Q. PP/Clay nanocomposites prepared by grafting–melt intercalation. *Polymer,* **2001***, 42*, 10013-10019.

[4] Reichert, P.; Nitz, H.; Klinke, S.; Brandsch, R.; Thomann, R.; Mulhaupt, R. Poly (propylene)/organoclay nanocomposite formation: Influence of compatibilizer functionality and organoclay modification. *Macromol. Mater. Eng.,* **2000***, 275(2)*, 8-17.

[5] Hasegawa, N.; Kawasumi, M.; Kato, M.; Usuki, A.; Okada, A. Preparation and mechanical properties of polypropylene-clay hybrids using a maleic anhydride-modified polypropylene oligomer. *J. Appl. Polym. Sci.,* **1998***, 67*, 87-92.

[6] Zhao, Z.; Tang, T.; Qin, Y.; Huang, B. Effects of surfactant loadings on the dispersion of clays in maleated polypropylene. *Langmuir,* **2003***, 19*, 7157-7159.

[7] Pozsgay, A.; Frater, T.; Szazdi, L.; Muller, P.; Sajo, I.; Pukanszky, B. Gallery structure and exfoliation of organophilized montmorillonite: Effect on composite properties. *Eur. Polym. J.,* **2004***, 40*, 27-36.

[8] Zheng, W.; Lu, X.; Toh, C.; Zheng, T.; He, C. Effect of clay on polymorphism of polypropylene in Polypropylene /Clay nanocomposites. *J. Appl. Polym. Sci: Part B: Polym. Phys.*, **2004***, 42*, 1810-1816.

[9] Modesti, M.; Lorenzetti, A.; Bon, D.; Besco, S. Effect of processing conditions on morphology and mechanical properties of compatibilized polypropylene nanocomposites. *Polymer,* **2005***, 46*, 10237-10245.

[10] Wu, J.; Wu, T.; Chen, W.; Tsai, S.; Kuo, W. Preparation and characterization of PP/Clay nanocomposites based on modified polypropylene and clay. *J. Polym. Sci: Part B: Polym. Phys.,* **2005** *43*, 3242-3254.

[11] Morlat, S.; Mailhot, B; Gonzalez, D.; Gardette, J. Photo-oxidation of polypropylene/montmorillonite nanocomposites. 1. Influence of nanoclays and compatibilizining agent. *Chem. Mater.,* **2004***, 16*, 377-383.

[12] Szazdi, L.; Pukanszky Jr, B.; Foldes, E.; Pukanszky, B. Possible mechanism of intercalation among the components in MAPP modified layered silicate PP nanocomposites. *Polymer,* **2005***, 46*, 8001-8010.

[13] Ding, C.; Jia, D.; He, H.; Guo, B.; Hong, H. How organomontmorillonite truly affects the structure and properties of polypropylene. *Polym. Test.,* **2005***, 24*, 94-100.

[14] Ratnayake, U.; Howorth, B. Polypropylene-clay nanocomposites: Influence of low molecular weight polar additives on intercalation and exfoliation behavior. *Polym. Eng. Sci.,* **2006***, 1008-1015.

[15] Zhang, Q.; Fu, Q.; Jiang, L.; Lei, Y. Preparation and properties of polypropylene /montmorillonite layered nanocomposites. *Polym. Int.,* **2000***, 49*, 1561-1564.

[16] Korakianiti, A.; Papaefthimiou, V.; Daflou, T.; Kennou, S.; Gregriou, V. Characterization of Polypropylene (PP) Nanocomposites for Industrial Applications. *Macromol. Symp.,* **2004***, 205*, 71-84.

[17] Chiu, F.; Lai, S.; Chen, J.; Chu, P. Combined effects of clay modifications and compatibilizers on the formation and physical properties of melt-mixed polypropylene/clay nanocomposites. *J. Appl. Polym. Sci: Part B: Polym. Phys.*, **2004***, 42*, 4139-4150.

[18] Bohning, M.; Goering, H.; Fritz, A.; Brzezinka, K.; Turky, G.; Schonhals, A.; Schartel, B. Dielectric study of molecular mobility in poly (propylene-graft-maleic anhydride)/clay nanocomposites. *Macromolecules,* **2005***, 38*, 2764-2774.

[19] Wang, Y.; Huang, S.; Guo, J. The state of clay dispersion in maleated polypropylene /organoclay nanocomposites *via* dielectric spectroscopy measurements. *e-Polymer*, **2008***, 75*, 1-16.

[20] Wang, Y.; Huang, S. Solution intercalation and relaxation properties of maleated polypropylene/ Organoclay Nanocomposites. *Polym.-Plast. Technol. Eng.*, **2007***, 46*, 1039-1047.

[21] Kalgaonkar, R.; Jog, J. Molecular dynamics of copolyester/clay nanocomposites investigated by viscoelestic and dielectric analysis. *J. Polym. Sci: Part B: Polym. Phys.*, **2008***, 46*, 2539-2555.

[22] Chanmal, C.; Jog, J. Study of dielectric behavior in PVDF/Clay nanocomposites. *e-Polymers*, **2009***, 112*, 1-8.

[23] Akinci, A. Mechanical and structural properties of polypropylene composites filled with graphite flakes. *Mater. Sci. Eng.*, **2009***, 35/2*, 91-94.

[24] Galgali, G.; Ramesh, C.; Lele, A. A Rheological study on the kinetics of hybrid formation in polypropylene nanocomposites. *Macromolecule,* **2001***, 34, 852*-858.

[25] Hambir, S.; Bulakh, N.; Kodgire, P.; Kalgaonkar, K.; Jog, J. PP/Clay nanocomposites: A study of crystallization and dynamic mechanical behavior. *J. Polym. Sci: Part B: Polym. Phys.,* **2001***, 39*, 446-450.

[26] Dong, Y.; Bhattacharyya, D.; Hunter, P. Experimental characterization and object-oriented finite elemental modeling of polypropylene /organoclay nanocomposites. *Composit. Sci. Technol.*, **2008***, 68*, 2864-2875.

[27] Hong, P.; Chuang, W.; Yeh, W.; Lin, T. Effect of rigid amorphous phase on glass transition behavior of poly (trimethylene terepyhalate). *Polymer,* **2002***, 43*, 6879-6886.

[28] Lu, H.; Nutt, S. Restricted relaxation in polymer nanocomposites near glass transition. *Macromolecules,* **2003***, 36,* 4010-4016.

[29] McCrum, N.; Read, B.; Williams, G. *Anelastic and Dielectrical effects in polymeric solids.* John Willey and Sons: USA **1967**.

[30] Kremer; K.; Schonhals, A. *Broadband Dielectric Spectroscopy*. Springer: USA **2003**.

[31] Lee, Y.; Bur, A.; Roth, S. Correlation between degree of exfoliation, dielectric properties and light transmission of nylon 11/clay nanocomposites probed by an online dielectric slit die. Proceeding of Society of Polymer Engineers: Annual Technical conference. *ANTEC,* **2004***, Vol. 1 (Processing)*, pp. 1279-1283.

[32] Page, K.; Adachi, K. Dielectric relaxation in montmorillonite/polymer nanocomposites. *Polymer,* **2006***, 47, 6406-6413*.

[33] Mijovic, J.; Lee, H.; Kenny, J.; Mays, J. Dynamics in polymer-silicate nanocomposites as studied by dielectric relaxation spectroscopy and dynamic mechanical spectroscopy *Macromolecules,* **2006***, 39*, 2172-2182.

[34] Motori, A.; Montanari, G.; Saccani, A.; Patuelli, F. Electrical conductivity and polarization processes in nanocomposites based on isotactic polypropylene and modified synthetic clay. *J. Polym. Sci: Part B: Polym. Phys.*, **2007***, 45,705*-713.

[35] Boyd, R.; Hasan, A. Aliphatic polyesters as models for relaxation processes in crystalline polymers: 4. dielectric relaxation in oriented specimens. *Polymer,* **1984***, 25*, 347-356.

[36] Kalakkunnath, S.; Kalika, D. Dynamic mechanical and dielectric relaxation characteristics of poly (trimethylene terephthalate). *Polymer*, **2006***, 47*, 7085-7094.

[37] Shafee, E. The influence of semicrystalline morphology on the dielectric relaxation properties of poly (3-hydroxybutyrate). *Eur. Polym. J.,* **2007***, 37,* 1677-1584.